

1 A novel method for image thresholding using interval
2 type-2 fuzzy set and Bat algorithm

3 Soumyadip Dhar^a, Malay K. Kundu^b

4 ^a*RCCIT, Kolkata-700015, India, rccsoumya@gmail.com*

5 ^b*ISI, Kolkata-700108, India, malay@isical.ac.in*

6 **Abstract**

In this paper, we propose a novel image thresholding method based on the interval type-2 fuzzy set (IT2FS). The interval type-2 fuzzy membership function (IT2FMF) is generated from a bag of type-1 fuzzy membership functions (T1FMFs) chosen adaptively based on the image characteristics for a given problem. An evolutionary algorithm called Bat algorithm is used to enhance the computational efficiency of the proposed thresholding technique. It is expected that the IT2FS based threshold technique will be better than that of the methods based on type-1 fuzzy set due to superior uncertainty handling capacity of the former technique. This fact is experimentally verified using benchmark dataset. The performance and robustness of the proposed method under different noise corruptions are measured statistically on the dataset by Modified Cramer-Rao Bound. The segmentation performance of the proposed method is compared experimentally with that of the state-of-the-art methods based on fuzzy and non-fuzzy frameworks. It is observed that the proposed method can achieve a higher segmentation accuracy in comparison to other state-of-the-art methods when they are benchmarked against the Modified Cramer-Rao Bound. Also, on average the misclassification error (ME) of the proposed method in segmentation is found to be minimum in comparison to the state-of-the-art methods.

7 *Keywords:* Interval type-2 membership function, uncertainty handling, image
8 thresholding, Bat algorithm, Modified Cramer-Rao Bound.

9 1. Introduction

10 Image thresholding is one of the most commonly used methods of two class ob-
11 ject background segmentations. In a two class image segmentation process based on
12 thresholding, it is expected that the process should be capable of making two distinct
13 regions. The regions should be made in such a way that their within class variation
14 is negligible in comparison to across the region variations. Also, the location of the
15 boundary between the two regions should be as accurate as possible. In order to locate
16 the segmentation boundary accurately, it is necessary that the process should be capa-
17 ble of reducing uncertainty arising due to gray level and spatial ambiguity in an image.
18 The ambiguities occur as a result of digitization with finite steps. The segmentation
19 using thresholding is one of the basic step of image analysis having a wide variety of
20 applications for non-destructive testing, text binarization, medical image processing
21 etc. Various applications of thresholding can be found in [1].

22 The literature on the approaches used for finding accurate threshold value in a seg-
23 mentation process is quite rich. Conventional thresholding methods without the un-
24 certainty handling capacity can be classified mainly into two categories, parametric
25 and nonparametric methods[2]. Parametric methods [3, 2] assume a statistical distri-
26 bution associated with the gray level of each class. On the contrary, nonparametric
27 methods [4, 5, 6, 7, 8, 9, 10, 11] are distribution-free approaches and they determine
28 the optimal threshold by optimizing certain objective function. The non-parametric
29 method by Kundu et al. [12] used human psychovisual phenomena (HVS) for thresh-
30 old selection.

31 Both the conventional parametric and non-parametric methods involve crisp deci-
32 sion (i.e yes or no, black and white, 0 and 1 etc) about the object and background
33 regions. They ignore the uncertainties present in a digital image due to gray level and
34 spatial ambiguity in the image. So their performance becomes poor when the bound-
35 aries between the regions are not distinct (abrupt change), rather it changes gradually
36 from one region to another (slant change). In view of that, uncertainty handling model
37 based on fuzzy set as introduced by Zadeh [13] becomes a popular tool for segmenta-
38 tion applications. Pal et al. [14, 15] used fuzzy entropy method for thresholding and

39 image enhancement. Also Ye et al. [16] and Huang et al. [17] proposed the fuzzy en-
40 tropy based thresholding algorithm where they minimized the entropy to obtain the
41 threshold value. Different methods using the fuzzy set for image thresholding were
42 also proposed in [18] and [19].

43 In a conventional fuzzy set, which is also called a type-1 fuzzy set, each element
44 can have any membership value between 0 and 1. In the true sense of fuzzy set as a tool
45 for uncertainty handling, the membership value should also be a fuzzy number. Since
46 the type-1 membership values are totally crisp, the type-1 set does not follow the ideal
47 property of a true uncertainty handling mechanism. This problem is the motivation
48 behind the concept of type-2 set as an extension of the type-1 fuzzy set (T2FS) [20].
49 In a type-2 fuzzy set, the uncertainty at a point is represented by a range of values
50 rather than a single value. The range of values is called the primary memberships of
51 the point. Again, each point in the range of values has its own membership values
52 called the secondary membership. Although type-2 fuzzy sets can give more freedom
53 to the decision-making process, but three-dimensional natures of the type-2 member-
54 ship functions make them very difficult to compute practically [21, 22]. Due to the
55 complex nature of type-2 fuzzy sets, interval type-2 fuzzy sets (IT2FS) are introduced
56 as a practical extension of general type-2 fuzzy sets, with a uniform secondary mem-
57 bership function [23]. Tizhoosh [24] proposed an image thresholding method using
58 interval type-2 set and a measure of ultrafuzziness. Pagola et al. [25] proposed an ap-
59 proach for estimating the IT2FMF from a group of conventional type-1 membership
60 functions and used it for the image thresholding applications.

61 Though many researchers used the IT2FMF for image segmentation, in any IT2FMF
62 the main concern is to find the proper intervals associated with it. The researchers
63 estimated the intervals associated with the IT2FMF by various methods. Tizhoosh
64 [24] generated the intervals by blurring a type-1 membership function. Obviously, the
65 accuracy of the IT2FMF depended on the particular membership function i.e on the
66 opinion of the expert. That means, the choice of T1FMF for generating IT2FMF is
67 individualistic or ad-hoc. Again, the blurring operation may lead to disappointing re-
68 sults [26]. On the other hand, Pagola et al. [25] combined the opinion of different
69 experts (i.e different type-1 membership functions) to develop the IT2FMF. Here, the

70 intervals were generated due to the difference of opinions between the experts. Tahayori
71 et al. [27] used fuzzy information-theoretic kernels for generating the IT2FM from a
72 set of T1MFs. A procedure for generating a set of extended IT2FMs from data for
73 an interval type-2 linguistic variable was proposed by Liao [28]. Here, the parameters
74 of the IT2FMF were obtained by minimizing the mean squared error (MSE) between
75 the membership values obtained by fuzzy c-means variant (FCMV) [29] and those pre-
76 dicted by the extended IT2MFs. Ideally, for reducing uncertainty in locating the seg-
77 mentation boundary, one should also consider the statistics of the image at hand for
78 computing the IT2FMF. That means the intervals associated with it should be esti-
79 mated adaptively. This shot of adaptation for computing the IT2FMF have not been
80 followed by any other researchers including Tizhoosh and Pagola. Rather, they pre-
81 assumed the intervals independent of the image at hand. Hence, they required opinions
82 of the external experts. This is the motivation behind our current investigation to gen-
83 erate IT2FMF adaptively to find a proper threshold value. This would be based on an
84 accurate and exact estimation of an IT2FMF adaptively from a bag which contains dif-
85 ferent T1MFs. The bag of type-1 membership functions is used, as we do not know
86 the suitable function for the particular image at hand. To select the proper set of mem-
87 bership functions efficiently from the bag, we have to use an evolutionary algorithm
88 in the proposed method. Similar methodology can be used for generating the extended
89 IT2MFs proposed by Liao [28] depending on the image at hand for image thresholding
90 application.

91 Nowadays, apart from genetic algorithm [30], several evolutionary algorithms have
92 been used by researchers for optimization [31, 32, 33, 34]. In the proposed method,
93 we use nature inspired Bat Algorithm (BA), a relatively new stochastic evolutionary
94 algorithm [35] for this search operation. The BA has gained popularity due to its ca-
95 pability of handling the optimization problem more efficiently than other evolutionary
96 algorithms [36, 16]. The BA algorithm has been used in many optimization problem
97 applications and can be found in [37].

98 The paper is organized as follows. Section 2 describes the proposed method and
99 novelty of the proposed method. Section 3 describes the different type-1 membership
100 functional forms used for generation of IT2FMF and image thresholding. The theory

101 of interval type-2 fuzzy set and the measure of uncertainty are described in Section
102 4. The theory of quantitative performance measure and modified Cramer-Rao bound is
103 discussed in Section 5. The procedure for generating interval type-2 fuzzy membership
104 function from a bag of type-1 membership functions are described in Section 6 . The
105 optimization problem and the theory of Bat algorithm are discussed in Section 7. The
106 implementation of an efficient approach to generate the IT2FMF for thresholding are
107 discussed in Section 8. Section 9 describes the results, comparison with state-of-the-art
108 methods and the statistical measure of the performance.

109 **2. Proposed method**

110 Here we propose an image thresholding method based on IT2FS with adaptive
111 estimation of the IT2FMF. The uncertainty in the image is reduced to get the optimal
112 threshold value by minimizing the IT2FS entropy. The exact IT2FMF is obtained when
113 interval type-2 fuzzy entropy produces the minimum value i.e the IT2FS with minimum
114 uncertainty. In our method, for building the IT2FS, the intervals of the IT2FMF are es-
115 timated from a combination of a bag of type-1 membership functions depending on the
116 image statistics. These membership functions are generally used for image threshold-
117 ing, but all the functions are not suitable for a particular image at hand. Naturally, the
118 exact IT2FMF depends on the suitability of the type-1 membership functions and the
119 corresponding parameters associated with them for the image at hand.

120 The whole operation of generating the IT2FMF for thresholding involves the search
121 of a proper combination of T1FMFs with the corresponding optimal set of parameters.
122 The parameters should be optimal in the sense that they should generate the IT2FMF
123 with minimum uncertainty. The parameters are discrete real variables or integers which
124 are bounded within a range. So, to get an optimal parameter set, we have to search from
125 a large combinations of real or integer values within the range. Thus, the search op-
126 eration is computationally expensive. To reduce the computational complexity and in-
127 crease the efficiency of the search operation, we have to use an evolutionary algorithm
128 to find the optimal set of parameters with real or integer values [38]. As the search
129 involves the minimization of uncertainty, the interval type-2 function entropy function

130 would be the objective function. The schematic diagram of the proposed method is
131 shown in Figure 1.

132 2.1. Novelty of the proposed method

133 The novelties of the proposed method are described below

134 **(1)** : In a conventional fuzzy set, choice of the membership function is individualistic
135 or ad-hoc. So there may be a quite substantial error in the measure of uncertain-
136 ties. To reduce the error it is desirable to adopt a mechanism so that the most
137 suitable membership function can automatically be selected. That mechanism
138 is proposed while computing appropriate IT2FMF by automatic means from a
139 bag of type-1 membership functions, depending on the image statistics. This is
140 implemented by proposing a suitable algorithm based on evolutionary Bat al-
141 gorithm for choosing appropriate T1FMFs with suitable parameter values. The
142 technique greatly reduces the error in uncertainty representation and increases
143 the accuracy of thresholding as evident from the results.

144 **(2)** : In the proposed method the IT2FMF is a combination of a bag of T1FMFs.
145 Hence, it also reduces the the uncertainties due to gray level and spatial ambigu-
146 ities in an image like conventional type-1 fuzzy set.

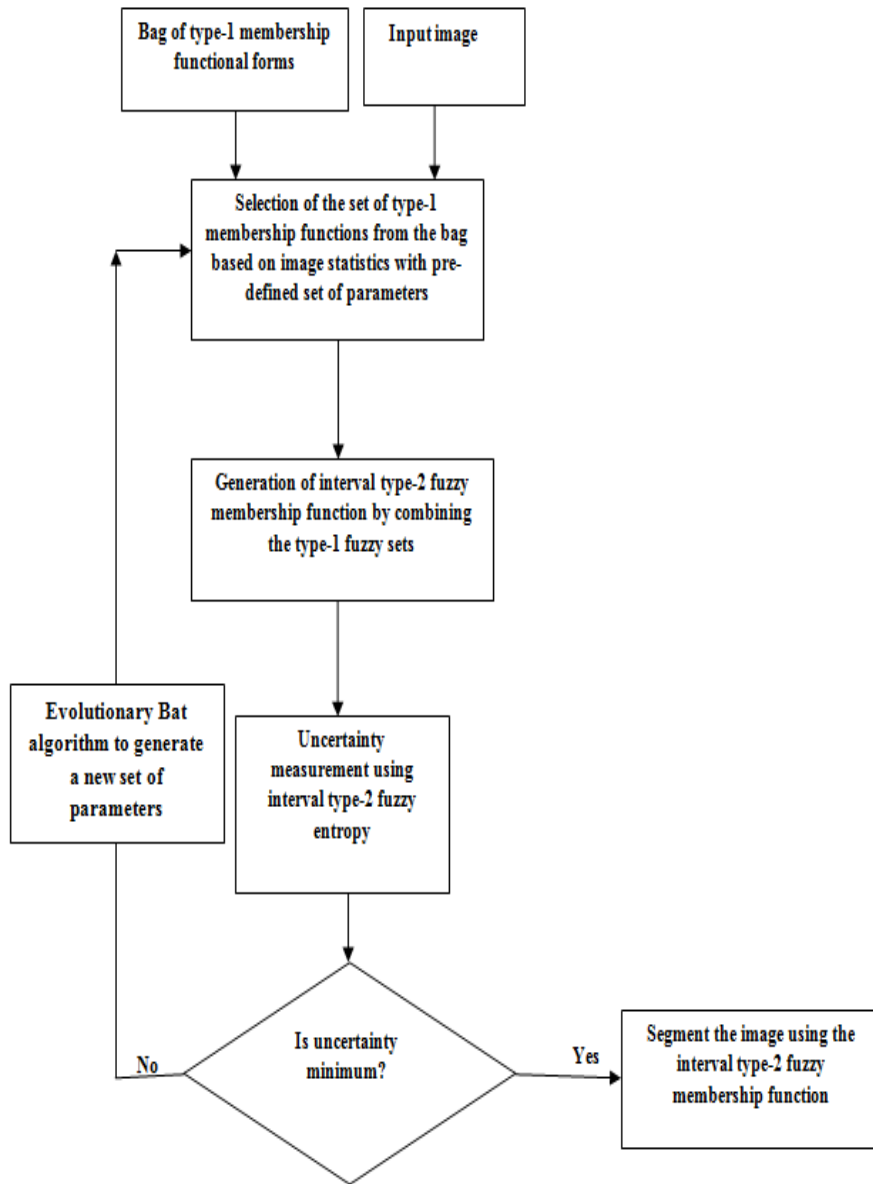


Figure 1: Schematic diagram of the proposed method.

147 **3. Various models of type-1 membership functional forms used for generation of**
 148 **interval type-2 membership functions:**

149 There are several type-1 membership functional forms which are commonly used
 150 for generating type-2 membership functions. In the proposed method the bag contains
 151 the four functions. These four types of membership functions also segment the object
 152 and background of an image. The four functions are described below.

153 1) Restricted Equivalence function (REF): REF function was proposed by Bustince et
 154 al. [39]. A function $REF : [0, 1]^2 \rightarrow [0, 1]$ is defined as

155 (1) $REF(x, y) = REF(y, x)$ for all $x, y \in [0, 1]$

156 (2) $REF(x, y) = 1$ if and only if $x = y$

157 (3) $REF(x, y) = 0$ if and only if $x = 1$ and $y = 0$ or $x = 0$ and $y = 1$

158 (4) $REF(x, y) = REF(c(x), c(y))$ for all $x, y \in [0, 1]$, c being a strong negation

159 (5) For all $x, y, z \in [0, 1]$ if $x \leq y \leq z$, then $REF(x, y) \geq REF(x, z)$ and $REF(y, z) \geq$
 160 $REF(x, z)$

161 The membership function by REF is

$$\mu_1(q) = \begin{cases} (REF\left(\frac{q}{L-1}, \frac{m_b(t)}{L-1}\right)) & \text{if } q \leq t \\ (REF\left(\frac{q}{L-1}, \frac{m_o(t)}{L-1}\right)) & \text{if } q > t \end{cases} \quad (1)$$

162 $REF(x, y) = 1 - |x - y|^{k1}$ Here $m_b(t) = \frac{\sum_{q=0}^t qh(q)}{\sum_{q=0}^t h(q)}$, $m_o(t) = \frac{\sum_{q=t+1}^L qh(q)}{\sum_{q=t+1}^L h(q)}$

163 The generation of optimal threshold point from the type-1 fuzzy sets of REF is
 164 very simple and time efficient [40]. L denotes the level of pixels and $h(q)$ denotes the
 165 frequency of the pixel with intensity q and $k1 > 0$. The threshold value is denoted by t .

166 2) Membership functions proposed by Huang [17]:

$$\mu_2(q) = \begin{cases} \frac{1}{1+(|q-m_b(t)|/C)^{k2}} & \text{if } q \leq t \\ \frac{1}{1+(|q-m_o(t)|/C)^{k2}} & \text{if } q \geq t \end{cases} \quad (2)$$

167 where $k2 > 0$ and C is the constant and its value is taken as 20 in the proposed method.

168 3) Membership function used by Tizhoosh : This membership function defined in [24]

169 as

$$\mu_3(q) = \begin{cases} 1 - \left(\frac{q}{t}\right)^{k3} & \text{if } q \leq t \\ 1 - \left(\frac{L-q}{L-t}\right)^{k4} & \text{if } q \geq t \end{cases} \quad (3)$$

170 where $k_3, k_4 > 0$.

171 4) Exponential membership function: The exponential membership function for thresh-
172 olding is given by

$$\mu_4(q) = \begin{cases} e^{-\left(\frac{|q-m_p(t)|}{L}\right)^{k_5}} & \text{if } q \leq t \\ e^{-\left(\frac{|q-m_o(t)|}{L}\right)^{k_5}} & \text{if } q \geq t \end{cases} \quad (4)$$

173 where $k_5 > 0$.

174 The range of the k_1, k_2, k_3, k_4, k_5 are shown in Section 7.1.

175 All the membership functions above perform the segmentation operation. But, dif-
176 ferent membership functions produce different membership values for the same inten-
177 sity value. Hence, different membership values give the different type-1 fuzzy set for
178 the same image. Obviously, each of the type-1 fuzzy set does not produce the desired
179 segmentation result where uncertainty is represented by a single point which depends
180 on a single membership function. Since it is very difficult to decide the exact T1FMF,
181 it is better to define a fuzzy set which is made up from more than one T1FMFs. Hence,
182 we use a bag of functions rather than a single function. Here, the intervals of the
183 IT2FMF are originated due to the difference of the membership values of a pixel by
184 the type-1 membership functions. More the interval, the higher will be the uncertainty.
185 Hence, it represents the uncertainty due to different membership values. Also, each
186 T1FMF value represents the uncertainty present in the image.

187 In the next two sections, we will discuss the theory of IT2FS and the theory of per-
188 formance measure of the proposed method.

189

190 4. Interval type2 fuzzy sets :

191 4.1. Interval type-2 fuzzy membership functions

192 In a type-2 fuzzy set(T2FS), the MF(membership function) is itself fuzzy[20]. A
193 type-2 set denoted by \tilde{A} is characterized by type-2 membership function $\mu_{\tilde{A}}(x, u)$,
194 where $x \in X$,i.e

$$\tilde{A} = \{(x, u), \mu_{\tilde{A}}(x, u) | \forall x \in X, \forall u \in J_x \subseteq [0, 1]\} \quad (5)$$

195 in which $0 \leq \mu_{\tilde{A}}(x, u) \leq 1$. \tilde{A} can also be expressed as

$$\tilde{A} = \int_{x \in X} \int_{u \in J_x} \mu_{\tilde{A}}(x, u) / (x, u), J_x \subseteq [0, 1] \quad (6)$$

196 where $\mu_{\tilde{A}}(x, u)$ is the secondary membership function and J_x is the primary mem-
 197 bership of x which is the domain of secondary membership function. Here $\int \int$ de-
 198 notes union over all admissible x and u . For discrete universes of discourse \int is de-
 199 noted by \sum . When all $\mu_{\tilde{A}}(x, u) = 1$ in the Eq.6, then \tilde{A} becomes interval type-2 fuzzy
 200 set(IT2FS) [26]. That means in IT2FMF, the secondary grade which is the ampli-
 201 tude of secondary MF becomes one. Uncertainty in the primary membership of an
 202 interval type-2 fuzzy set \tilde{A} , consists of a bounded region called the footprint of uncer-
 203 tainty(FOU). It is the union of all primary membership, i.e.

$$FOU(\tilde{A}) = \bigcup_{x \in X} J_x \quad (7)$$

204 As secondary grades of IT2FS carry no new information, the FOU is a complete de-
 205 scription of an IT2FS. The upper membership function (UMF) and lower membership
 206 function(LMF) of \tilde{A} are two T1FMFs that bound the $FOU(\tilde{A})$. The UMF denoted by
 207 $\overline{\mu}_{\tilde{A}}(x), \forall x \in X$ is associated with the upper bound of $FOU(\tilde{A})$ and LMF denoted by
 208 $\underline{\mu}_{\tilde{A}}(x), \forall x \in X$ is associated with the lower bound of $FOU(\tilde{A})$. Mathematically they can
 209 be expressed as

$$\overline{\mu}_{\tilde{A}}(x) \equiv \overline{FOU(\tilde{A})} \forall x \in X \quad (8)$$

210

$$\underline{\mu}_{\tilde{A}}(x) \equiv \underline{FOU(\tilde{A})} \forall x \in X \quad (9)$$

211 In IT2FS J_x can be expressed as

$$J_x = \{(x, u) : u \in [\underline{\mu}_{\tilde{A}}(x), \overline{\mu}_{\tilde{A}}(x)]\} \quad (10)$$

212 and $FOU(\tilde{A})$ can be expressed as

$$FOU(\tilde{A}) = \bigcup_{x \in X} [\underline{\mu}_{\tilde{A}}(x), \overline{\mu}_{\tilde{A}}(x)] \quad (11)$$

213 The footprint of uncertainty is very important for an interval type-2 fuzzy membership
 214 representation. Shape of FOU not only represents the nature of the uncertainties but

215 also provides a very verbal description of the entire domain of support for all secondary
 216 grades of an interval type-2 membership function.

217

218 4.1.1. Uncertainty measure in IT2FS

219 In IT2FS, the FOU represents the uncertainty present in the set. In the FOU, the
 220 lower membership function $\underline{\mu}_{\tilde{A}}$ and upper membership function $\overline{\mu}_{\tilde{A}}(x)$ play an im-
 221 portant role for uncertainty measure in IT2FS. In this paper, we use the uncertainty
 222 measure proposed by Kacprzyk and Smidtz [41]. It is defined as

$$\xi_k(\tilde{A}) = \frac{1}{N} \sum_{i=1}^N \frac{1 - \max(1 - \overline{\mu}_{\tilde{A}}(x), \underline{\mu}_{\tilde{A}}(x))}{1 - \min(1 - \overline{\mu}_{\tilde{A}}(x), \underline{\mu}_{\tilde{A}}(x))} \quad (12)$$

223 Where N is the cardinality of the fuzzy set.

224 5. Performance measure of the proposed method

225 5.1. Misclassification Error(M.E)

226 The quantitative performance of the proposed thresholding method and all the
 227 methods compared here are measured using widely used segmentation evaluation met-
 228 ric called Misclassification error [1] which is given by

229

$$M.E = 1 - \frac{|T_o \cap T_t| + |G_o \cap G_t|}{|T_o| + |G_o|} \quad (13)$$

230 where B_o and F_o denotes the background and foreground of the original image(ground
 231 truth). B_T and F_T denotes the background and foreground of the tested image. The $|\cdot|$ is
 232 the cardinality of the set. M.E nearer to 1 means wrongly classified image and nearer
 233 to 0 means correct classification.

234 Though we measure the performance of all the methods considered here using M.E,
 235 one can find in [42, 43] that performance of segmentation evaluation methods varies
 236 widely depending on image content. Therefore it is better to find out the statistical per-
 237 formance bound of segmentation methods associated with a particular image content.
 238 The bound should indicate the maximum achievable performance of a segmentation
 239 algorithm on the particular image. Hence, to statistically bound the performance of

240 our image thresholding method a modified Cramer-Rao bound(CRB) on Mean Square
 241 Error(MSE) for segmentation proposed by Peng et al. [44] was used. In the next sub-
 242 section, we discuss it.

243 5.2. The modified Cramer-Rao bound for MSE:

244 For finding the modified Cramer-Rao bound of the MSE we adopt the procedure
 245 in [44] where it is assumed that the output pixel level of a segmentation algorithm is a
 246 biased estimate of true pixel level. To determine the MSE bound for the test image, the
 247 segmentation problem is first modeled using varying-coefficient model(VCM) [44].
 248 In this model the pixel intensity value $y(x)$, where x are the pixel indices and ordered
 249 through zig-scanning, starting from top left to bottom right of an image with N pixels
 250 can be represented as

$$y(x) = \mathbf{h}^T \cdot \boldsymbol{\varphi}(x; \mathbf{B}) + w(x) \quad (14)$$

251 Where T denotes the transpose of matrix. Here pixel intensity $y(x)$ includes the con-
 252 tribution from all the basis regions in an image i.e the regions that cannot be further seg-
 253 mented. The $w(x)$ represents the noise in the image. The $\mathbf{h}(x) = [h_1(x), h_2(x) \dots h_M(x)]^T$, where
 254 an image is divided into M basic regions and $h_i(x)$ is the membership value of x in
 255 i th basic region. This membership value can be interpreted as the degree to which
 256 the pixel x belongs to the i th basic region $\boldsymbol{\varphi}(x; \mathbf{B}) = [\varphi(x; \beta_1), \varphi(x; \beta_2), \dots, \varphi(x; \beta_M)]$,
 257 $\varphi(x; \beta_1)$ represents the intensity of pixel at i th region and $\mathbf{B} = [\beta_1^T, \beta_2^T, \dots, \beta_M^T]$. Here
 258 $\varphi(x; \beta_i) = \sum_{l=1}^m \beta_{il} \zeta_l(x)$ where $\zeta_l(x)$ are B-spline basis functions, β_i is the coefficient
 259 vector, m is the number of knots in the image and l is the index of the knots which are
 260 ordered through zig-scanning starting from top left to bottom right of an image. The
 261 MSE of an estimator $\hat{h}(x)$, which is the output membership value of a segmentation
 262 algorithm and biased estimator of the true pixel label $h(x)$ is given by

$$MSE = E(\|\hat{\mathbf{h}} - \mathbf{h}\|^2) \quad (15)$$

263 The Cramer-Rao bound for biased estimation of MSE [44]for an image is given by

$$\begin{aligned}
 CRB_{MSE} = & \frac{1}{MN} \sum_1^M Tr\{(E_{\mathbf{B}}[\mathbf{J}_F(\mathbf{h}_i)])^{-1} \\
 & - (E_{\mathbf{B}}[\mathbf{J}_F(\mathbf{h}_i)])^{-1} ((E_{\mathbf{B}}[\mathbf{J}_F(\mathbf{h}_i)])^{-1} + Cov(\mathbf{h}_i))^{-1} \\
 & ((E_{\mathbf{B}}[\mathbf{J}_F(\mathbf{h}_i)])^{-1})\} \quad (16)
 \end{aligned}$$

264 Where $Tr(\Gamma)$ represents the trace of the matrix Γ . Here $(E_{\mathbf{B}}[\mathbf{J}_F(\mathbf{h}_i)])$ denotes the ex-
 265 pectation of $\mathbf{J}_F(\mathbf{h}_i)$, where $\mathbf{J}_F(\mathbf{h}_i)$ is the Fisher information matrix of \mathbf{h}_i and $Cov(\mathbf{h}_i)$
 266 is the covariance of \mathbf{h}_i . Here we assume the estimator of \mathbf{h} to be biased and derive the
 267 bound on MSE of image thresholding results. The bound provides a valid performance
 268 prediction of the image thresholding algorithms and a benchmark of the thresholding
 269 results. The N is the number of the pixels in the image.

270 In the next section we will show the generation of IT2FMF from a bag of type-1
 271 membership functions.

272 6. Generation of interval type-2 membership function from a bag of type-1 mem- 273 bership functions:

274 Here we propose a method to generate an IT2FMF from a bag which has $n(n > 1)$
 275 number of type-1 fuzzy membership functions. That means, all the type-1 membership
 276 functions in the bag have contributions in making the IT2FS. For this, we follow the
 277 same strategy as used by Pagola et al. [25], but with the modification. Mathematically,
 278 here the IT2FS is expressed as

$$\tilde{A} : FS(X) \times FS(X) \dots n \text{ times} \rightarrow IT2FS(X) \quad (17)$$

279 Where $FS(X)$ is the type-1 fuzzy set and

$$\tilde{A}(\mu_1, \mu_2, \dots, \mu_n)(x) = \{x, [\underline{\mu}(x), \bar{\mu}(x)] | x \in X\} \quad (18)$$

280

$$\underline{\mu}(x) = t - norm(w_1\mu_1(x), w_2\mu_2(x), \dots, w_n\mu_n(x)) \quad (19)$$

281

$$\bar{\mu}(x) = t - conorm(w_1\mu_1(x), w_2\mu_1(x), \dots, w_n\mu_n(x)) \quad (20)$$

282 Here we use minimum t-norm and maximum t-conorm. The parameters w_1, w_2, \dots, w_n
 283 represent the weights of the membership functions under the constraint $\sum_{i=1}^n w_i = 1$.
 284 The interval $(\overline{\mu}(x) - \underline{\mu}(x))$ at x produces due to the difference between $\min(\mu_1(x), \mu_2(x), \dots, \mu_n(x))$
 285 and $\max(\mu_1(x), \mu_2(x), \dots, \mu_n(x))$. This interval represents the uncertainties at the point
 286 x . If we consider x to be a pixel intensity of an image then each of the $\mu_i(x)$ for
 287 $i = 1, \dots, n$ represents the uncertainty at x due to the gray level and spatial ambiguity
 288 of the image. Again the uncertainty at x due to different $\mu_i(x)$'s produces the interval
 289 $[\overline{\mu}(x) \quad \underline{\mu}(x)]$. When the length of the interval is high, uncertainty at the point x is high
 290 and vice versa.

291 In the proposed method we take $n = 4$ i.e the bag contains four type-1 membership
 292 functions. Though we use four different types of type-1 membership functions to gener-
 293 ate the IT2FMF, all of them are not equally important for a particular image. Since
 294 we do not know the exact function which will be suited for a given image, it seems ap-
 295 pealing and convenient to provide weights to each membership functions. Thus, four
 296 weight parameters w_1, w_2, w_3, w_4 are multiplied with μ_1, μ_2, μ_3 and μ_4 respectively .
 297 The weights are to be chosen according to the importance (suitability) of a function
 298 for a particular image and the weights depend on the particular image statistics. The
 299 combination should enable to generate the exact IT2FMF with minimum uncertainties.
 300 That means, the uncertainties will get minimized if the optimal set of parameters related
 301 with $\mu_1, \mu_2, \mu_3, \mu_4$, and w_1, w_2, w_3, w_4 are found. When the uncertainties are minimum,
 302 the image is segmented into object and background properly. The parameters have
 303 discrete integer or real values bounded within a range. So, finding the optimal set of
 304 parameters to generate the IT2FMF with minimum uncertainties is time-consuming.
 305 Thus, to speed up the process of generating the IT2FMF from the bag of type-1 mem-
 306 bership functions, we define an optimization problem. The optimization problem is
 307 solved by evolutionary Bat algorithm. In the next section, we will discuss the opti-
 308 mization problem to speed up the generation of the IT2FMF and the Bat algorithm.

309 7. Optimization problem and evolutionary Bat algorithm(BA)

310 7.1. Optimization problem

The optimization problem for generating the exact IT2FMF by the Eq(19) and Eq(20) with parameter set $p = (k_1, k_2, k_3, k_4, k_5, t, w_1, w_2, w_3, w_4)$ can be written as

$$\begin{cases} \text{Minimize : } \xi_k(\tilde{A}(x)) \text{ where } \tilde{A}(x) \text{ is an IT2FMF and it depends on parameter set } p, \\ \text{Subject to : } 0.40 \leq k_1 \leq 0.50, 2 \leq k_2, k_3, k_4 \leq 3, 1 \leq k_5 \leq 2, q_{min} \leq t \leq q_{max} \\ \text{and } \sum_{i=1}^4 w_i = 1 \text{ where } 0 \leq w_1, w_2, w_3, w_4 \leq 1 \end{cases}$$

311 where the q_{min} and q_{max} are minimum and maximum gray level intensity of the image.

312 In our proposed method we use the BA to solve the optimization problem. It is
 313 to be noted that though we choose the four functions mentioned in Section3, the pro-
 314 posed method can be applied to any other bag which contains any number of type-1
 315 membership functions ($n > 1$) and any set of type-1 membership functions. But, as
 316 more number of functions makes the procedure computationally more expensive and
 317 less number of functions may not represent the uncertainties properly, we are restricted
 318 to $n = 4$. In the following section, we will discuss the theory of BA in determining a
 319 optimal set of parameters.

320 7.2. Bat algorithm

321 7.2.1. Basic steps of Bat algorithm

322 Yang [35] invented a swarm intelligence optimization algorithm through simulat-
 323 ing the interesting behavior of a bat, which combines major advantages of simulated
 324 annealing and particle swarm optimization. Three generalized rules are used for im-
 325 plementing the bat algorithm:

- 326 1) All bats use echolocation to sense distance, and they also know the difference be-
 327 tween food/prey and background barriers. In echolocation system, bats emit high fre-
 328 quency and listen to returning echoes. The differences between the emitted frequencies
 329 and the echoed frequencies are used to determine the distance and location of the prey.
- 330 2) Bats fly randomly with velocity at a position with a fixed frequency, varying wave-
 331 length and loudness to search for prey. They can automatically adjust the wavelength

332 of their emitted pulses and adjust the rate of pulse emission depending on the proximity
333 of the target.

334 3) Although the loudness can vary in many ways, here it is assumed that the loudness
335 varies from a large (positive) to a minimum constant value.

336 Main steps of the algorithm [45] are given below

337 1) Initialization;

338 Repeat

339 2) Generation of new solutions;

340 3) Local searching;

341 4) Generation of a new solution by flying randomly;

342 5) Finding the current best solution; until requirements are met.

343 7.2.2. *Movements of virtual Bats*

344 In BA algorithm, initialization of the bat population is performed randomly. Gen-
345 erating new solutions are performed by moving virtual bats according to the following
346 equations:

$$f_i = f_{min} + (f_{max} - f_{min})\beta \quad (21)$$

347

$$v_i^t = v_i^{t-1} + (p_i^t - p^*)f_i \quad (22)$$

348

$$p_i^t = p_i^{t-1} + v_i^t \quad (23)$$

349 Where v_i^t and p_i^t represents the velocity and position of the i th bat at an iteration t .
350 The frequency of the bat is given by f_i . Initially, each bat is randomly assigned a
351 frequency f which is drawn uniformly from $[f_{min} \quad f_{max}]$. The $\beta \in [0 \quad 1]$ is a random
352 value drawn from a uniform distribution. Here p^* is the current global best location
353 (solution) which is located after comparing all the solutions among all the bats. After
354 the selection of a solution from the current best solutions, a new solution for each bat
355 is generated locally using a random walk according to the equation:

$$p_{new} = p_{old} + \eta A^t \quad (24)$$

356 Where $\eta \in [-1 \ 1]$ is a random number subject to Gaussian distribution. The η acts as
 357 a step size to generate new location (i.e new solution). The A^t is the average loudness
 358 of all the best solutions at this time step. The p_{old} is obtained from Eq23.

359 In the bat algorithm the loudness A_i and pulse rate emission r_i are updated at each
 360 iteration t . The loudness decreases when the bat finds the prey and the corresponding
 361 pulse emission increases. The loudness A_i and the rate of pulse emission r_i change
 362 according to the following equations.

$$A_i^{t+1} = \alpha A_i^t \quad r_i^{t+1} = r_i^0 [1 - e^{-\gamma}] \quad (25)$$

363 Where α and γ are constants and $0 < \alpha < 1$, $\gamma > 0$. When $t \rightarrow \infty$, $A_i^t \rightarrow 0$ and $r_i^t \rightarrow 0$.
 364 The α is similar to the cooling factor of a cooling schedule of a simulated annealing.
 365 The loudness and emission rate are updated only when the new solution is obtained,
 366 that means the bats move towards the optimal solution.

367 The update of the velocities and positions of bats have some similarity to the pro-
 368 cedure in the standard particle swarm optimization as f_i controls the pace and range
 369 of the movement of the swarming particles [35]. If we replace the variations of the
 370 frequency f_i by a random parameter and set $A_i = 0$ and $r_i = 1$, the bat algorithm essen-
 371 tially becomes the standard Particle Swarm Optimization (PSO) [35]. So, it can be said
 372 that BA is a generalized version of PSO and a balanced combination of the standard
 373 particle swarm optimization and simulated annealing.

374 8. Implementation

375 We have already stated that we used the BA to implement the generation of the
 376 IT2FMF from a bag of T1FMF depending on the image characteristics and define the
 377 optimization problem in Section 7.1. In the following subsections, we will discuss the
 378 parameters of the BA and the implementation of BA in determining the optimal set of
 379 parameters to generate the exact IT2FMF.

380 8.1. Representation of the parameters and domain of the parameters:

381 In BA each bat p_i , $i = 1, 2, \dots, n$ in the bat population is represented by a string of pa-
 382 rameters. Here in our method we have 10 parameters $(k_1, k_2, k_3, k_4, k_5, t, w_1, w_2, w_3, w_4)$

383 for the generating the IT2FMF. The domains of the ten parameters are shown in Sec-
 384 tion 7.1. Though an optimal solution in any evolutionary algorithm is obtained by an
 385 infinite number of population and an infinite number of generations, here for the prac-
 386 tical purpose we restricted to the initial bat population as 300 and the total number of
 387 iterations as 30.

388 *8.2. Reduction of the randomness of the parameters*

389 The uniform distribution is assumed when generating the initial population of the
 390 bats randomly. The parameters are bounded by some values (shown in Section 7.1).
 391 The values of the parameters (i.e the bat) outside the bound are the infeasible solution.
 392 But, the bound violation may occur due to the randomness of the parameters related
 393 to new solution generation, and random walk operation of the bats. To handle the
 394 randomness we use the strategy of repairing the bound violated parameters by Liao
 395 [38]. In this strategy, the parameter is repaired either by taking the bound value that is
 396 being violated or replacing it with a newly generated value within the bound.

397 *8.3. Evaluation function:*

398 We need an evaluation function to quantify the desired image thresholding result.
 399 The present algorithm considers the evaluation function as the fitness function of BA.
 400 Here use the interval type-2 fuzzy entropy given in the Eq.12 as an evaluation function.
 401 The entropy of an image X considers the global information and provides an average
 402 amount of fuzziness in the grayness of X, i.e., the degree of difficulty (ambiguity) in
 403 deciding whether a pixel would be treated as an object (dark) or a background (white).
 404 Therefore the concept of minimization of these ambiguity measures may be considered
 405 as the basis of a fitness (evaluation) function. The objective of the BA is to construct
 406 the exact IT2FMF with least entropy. So the entropy is used as the fitness function,
 407 where BA will try to find out the minimum value of it by tuning the parameters.

408 *8.4. An efficient approach for estimating the IT2FMF using Bat Algorithm :*

409 In our proposed method, the input image is first mapped into the type-1 fuzzy sets
 410 by a bag of T1FMFs with a set of parameters. The weights are assigned to the T1FMFs

Algorithm 1: Algorithm for efficient approach for estimating IT2FMF using Bat algorithm

Input: Image of dimensions $R \times S$, Four fuzzy type-1 membership functions $\mu_j, j = 1, 2, 3, 4$

Output: The IT2FMF with footprint of uncertainty and the segmentation result

Initialisation: Initialize the population of P bats i.e the set of position vectors

$p_i = (k_1, k_2, k_3, k_4, k_5, t, w_1, w_2, w_3, w_4)_i$. Also initialize the frequency f_i , the velocity v_i , the loudness A_i and pulse emission rate r_i where $i = 1, 2, \dots, P$. The maximum number of iterations is $M1$ and iteration number $iter = 0$.

- 1: **repeat**
- 2: **for** each bat p_i in the current population **do**
- 3: generate new solution i.e the new parameter vector by updating f_i , v_i and p_i with the help of p^* (Eq21, Eq22 and Eq23);
- 4: **if** ($rand > r_i$) **then**
- 5: select a local solution around the best solution. Here $rand$ is a random variable;
- 6: **end if**
- 7: Generate a new solution p_{inew} by flying randomly (Eq24);
- 8: Handle the bound violation by the parameters and map the image into T1FSs using p_{inew} and generate the IT2FMF from the T1FMFs $\mu_j, j = 1, 2, 3, 4$ by t-norm and t-conorm.(Eq19 and Eq20);
- 9: Calculate the evaluation function interval type-2 fuzzy entropy ξ_k .(Eq 12);
- 10: **if** ($rand < A_i$ and $\xi_k(p_{inew}) < \xi_k(p^*)$) **then**
- 11: Update the solution as $p_i = p_{inew}$ with increase of r_i and the decrease of A_i ;
- 12: **end if**
- 13: **end for**
- 14: $iter = iter + 1$;
- 15: Find the current best solution p^* with minimum entropy among all the bats in the current population;
- 16: **until** $iter = M1$ or no change in evaluation function
- 17: Return the IT2FMF, the FOU and the segmentation results by the parameter set of the best solution;

411 on the basis of the image statistics. The type-1 fuzzy sets are combined using t-norm
412 and t-conorm operations. The BA helps to speed the total process to find out the op-
413 timal combination which produces minimum interval type-2 fuzzy entropy. Thus the
414 IT2FMF maps the image pixels to IT2FS with least entropy and segments the image
415 into object and background.

416 In the proposed method, the BA tries to optimize the position of the virtual bat such
417 that it is nearer to the optimal solution (position). For this, the position, the velocity,
418 the frequency, the loudness and the pulse emission rate of bats in the population are ini-
419 tialized first. Each bat position p_i is a vector of the 10 parameters described in Section
420 7.1. For each position, the IT2FMF is produced. Then, the best position is found from
421 the bat population. Here, the best position is the position with minimum interval type-2
422 fuzzy entropy. It is followed by the process of making of the new solutions (positions)
423 for each bat, which are generated by adjusting the frequency, the velocity and using
424 the current best solution. The loudness and the pulse emission rate of each bat are also
425 updated. The process is repeated until it reaches the termination criteria. The current
426 best solution represents the optimal set of parameters of type-1 membership functions
427 to generate the IT2FMF. The step by step procedure is described in Algorithm 1.

428

429 **9. Experimental results & discussion:**

430 To illustrate the performance of the proposed method we tested our method on dif-
431 ferent types of images. We applied our method on the benchmark dataset of the camera
432 captured natural images from Weizmann [46], and Berkley [47]. Several nondestructive
433 tests(NDT) images from Mehmetsezgin [48] which were described in [1] were also
434 used for the experiment. The size of the images varies from 200×200 to 500×500 .
435 We compared the performance of proposed method both qualitatively and quantita-
436 tively with non-fuzzy statistical methods like Kapur [7], Otsu [4], Cai [5]; fuzzy type-1
437 entropy based method like Ye [16] and Hung [17] and interval type2 fuzzy methods of
438 Pagola [25] and Tizhoosh [24]. All the methods were performed using MATLAB2013
439 with 4GB RAM.

440 9.1. Quantitative estimation and accuracy of the proposed thresholding method

Table 1: Performance of different methods on 25 NDT images from [48]

Methods	Cai [5]	Kapur [7]	Otsu [4]	Huang [17]	Ye [16]	Tizhoosh [24]	Pagola [25]	Proposed
Average M.E	0.1132	.2042	0.2354	0.1969	0.0514	0.1418	0.1273	0.0480
Average Rank	3.73	5.82	6.37	5.402	2.77	4.95	4.73	2.23

441 For quantitative performance measure, we used NDT data set of 25 images from
 442 [48]. NDT means to detect an object and quantify its possible defects without harmful
 443 effects on it by special equipment and methods. An effective way to extract the regions
 444 is to find out proper threshold value of the image. For quantitative performance mea-
 445 sure, we took the average performance of 30 runs of the proposed Algorithm1. The
 446 average M.E(Eq13) and the average rank of the methods are shown in Table 1. For
 447 an image, the method with the lowest M.E was given rank 1 and all other ranks were
 448 calculated accordingly.

449 We also applied the eight methods on all the images of the data set [46]. The dataset
 450 contains 100 dissimilar natural scene images for two class segmentation. In Figure 2,
 451 the box plot diagram summarizes the Misclassification Error statistics of individual
 452 thresholding methods applied on the 100 images from[46]. It can be seen that the low-
 453 est median was achieved by the proposed method followed by Pagola and Cai. Also,
 454 the number of outlines of the proposed method was less compared to the other meth-
 455 ods. The interquartile range was also quite low for the proposed method.

456 It is observed from the table 1 and box plot in Figure2 that the quantitative per-
 457 formance of the proposed method, on average, was much better both on NDT and
 458 camera captured natural images, than that of the other seven methods compared here.
 459 The observation can be explained in the following way. The high uncertainties exist
 460 in the NDT images as their boundaries are not well defined. Similarly uncertainties
 461 present in camera captured natural scene due to digitization from analog domain. But
 462 the conventional nonparametric methods (Kapur, Otsu, and Cai) have no uncertainty
 463 handling capacities. So the hard decision about a pixel by the conventional methods

464 failed to produce the desired performance. Again, the fuzzy type-1 membership func-
465 tions of Ye and Huang could not represent the uncertainty properly with their crisp
466 membership values. Also, the choice of the membership functions of Huang was indi-
467 vidualistic, and it did not take into account the characteristics of the image at hand. So,
468 there were high chances of error in the representation of uncertainties. Though Ye used
469 Bat algorithm to find the proper type-1 membership function, the method lacked the
470 proper representation of uncertainty. Therefore, the method performed poorly on the
471 NDT images and the wide variety of images from [46]. On the contrary, the proposed
472 method has the uncertainty handling capacity of IT2FS based on the image statistics.
473 The importance of a T1FMF to estimate the IT2FMF for the image was determined
474 automatically by tuning the weight parameters. It is to be noted no prior knowledge
475 was provided about the image to estimate the IT2FMF. Tizhoosh used IT2FS for un-
476 certainty handling, but the IT2FMF was made by blurring a single type-1 membership
477 function and the intervals were pre-assumed. So the interval type-2 membership value
478 of the Tizhoosh mainly depended upon the corresponding type-1 membership function.
479 So, his type-2 membership function might not represent the uncertainties properly for
480 all types of images considered here. The IT2FMF used by Pagola was made from a
481 set of type-1 membership functions, but no criteria were given to select them for an
482 image at hand. So he ignored the image characteristics to generate the IT2FMF. Since
483 in our method the IT2FMF were computed adaptively based on the image statistics, the
484 proposed method outperformed both the Tizoosh and Pagola's method.

485

486 9.2. Statistical validation by the modified Cramer-Rao bound for MSE

487 To show the robustness of the proposed method under different noise corruptions,
488 we measured the lower bound for MSE on the NDT image dataset. Here we assumed
489 that each image included two non overlapping basic regions ($M = 2$), one was object
490 region and other was background region. The two regions were obtained from the
491 ground truth for the image provided in the dataset. The B-spline function used here
492 was the cubic B-spline. The knots were deployed at every 8 pixels in both horizontal
493 and vertical directions. White Gaussian noise was added to an image with zero mean

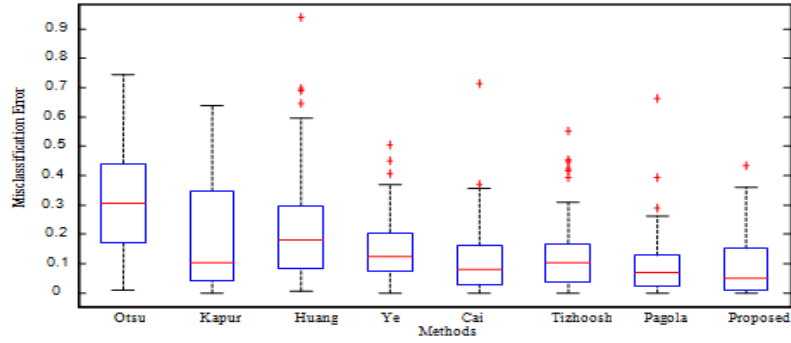
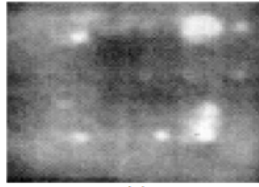
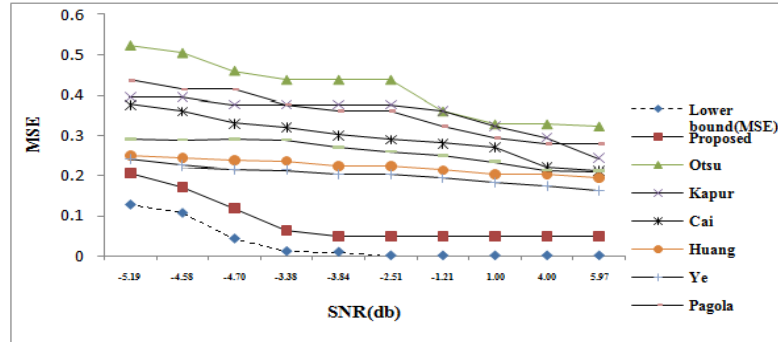


Figure 2: Box plots of Misclassification Errors of different methods on the data set [46].



(a)



(b)

Figure 3: (a) Original NDT test image from [48].(b) MSEs of various segmentation methods on the image at different SNRs and modified Cramer-Rao lower bound of MSE for the image.

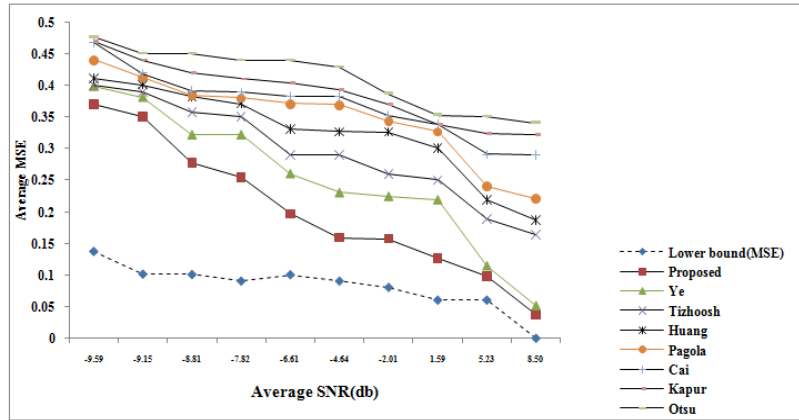


Figure 4: Average lower MSE bound and average MSEs of various methods at different average SNRs on the NDT images from [48].

494 and variance σ_2 . This procedure was used for all the 25 NDT data in the dataset. The
 495 MSE bound of a sample test image for the proposed method and all the methods compared
 496 here is shown in Figure 3. The lower bound indicates the maximum achievable
 497 segmentation performance for the particular image in terms of MSE. The average lower
 498 bound of MSE and average individual MSE at different SNRs are shown in Figure 4.
 499 From the result, it can be seen that the proposed method yielded better results in terms
 500 of smaller MSE, especially in the relatively higher SNRs followed by Ye. This mea-
 501 sure also indicates that the proposed method was more robust against the addition of
 502 noise compared to the other methods used here. The uncertainty increases in an image
 503 due to the addition of noise and the noise also changes the statistics of the image. As,
 504 in the proposed method the uncertainty was handled by adaptive IT2FS, the IT2FMF
 505 changed accordingly depending on the image statistics. So the method was more ro-
 506 bust against the noise than that of the other methods here. Also, the limitation of the
 507 proposed method and room for improvement against each SNR can also be seen from
 508 the graph.

509 9.3. Qualitative validation

510 In this subsection, we report the qualitative results to validate the quantitative es-
511 timations. For a test image, we show one qualitative result among the 30 runs of the
512 proposed Algorithm1. The qualitative result is the one which produced the minimum
513 M.E among the 30 runs of the algorithm. The intermediate and final interval type-2
514 membership functions (after 10,15 and 20 generations), corresponding upper member-
515 ship function, lower membership function, FOU(the black portion) and segmentation
516 result for a sample image is shown in Figure 5. The figure shows how the BA gradually
517 made the IT2FMF function. The FOU for each image represents the exact IT2FMF of
518 the image with least entropy generated by our method at the corresponding genera-
519 tions. The results also show the successive improvement of the segmentation results.
520 So, it can be said that the BA helped to reduce the uncertainties by generating the ex-
521 act IT2FMF. Some more results of segmentation by the proposed method, the exact
522 IT2FMF, histogram of the corresponding images and position of threshold point in the
523 histogram are shown in Figure6. It is clear from the image histograms that the valleys
524 were difficult to estimate. So it was difficult to locate the exact segmentation boundary,
525 but the visual inspection shows that our proposed method located the boundary prop-
526 erly. The segmentation results by the proposed method on an another set of images
527 are shown in Figure 7. The qualitative segmentation results of the NDT images by
528 eight different methods (Kapur [7],Otsu [4], Cai [5], Ye [16],Huang [17], Pagola [25],
529 Tizhoosh [24] and the proposed) are shown in the Figure 8. So, the results validated
530 the powerful uncertainty handling capacity of the IT2FS. Moreover, the uncertainties
531 arose due to the ambiguities present in a digital image and due to the opinion of differ-
532 ent experts (i.e different membership functions) were reduced by the proposed method
533 efficiently and adaptively. This shot of adaptation produced the proper threshold value
534 which was also the segmentation boundary between object and background. In the next
535 section, we tested the proposed method on the blurred images.

536 9.4. Result on blurred images

537 To verify the robustness of the proposed method, we have applied our method on
538 the blurred images. The images from [47], [48] and some images collected from the

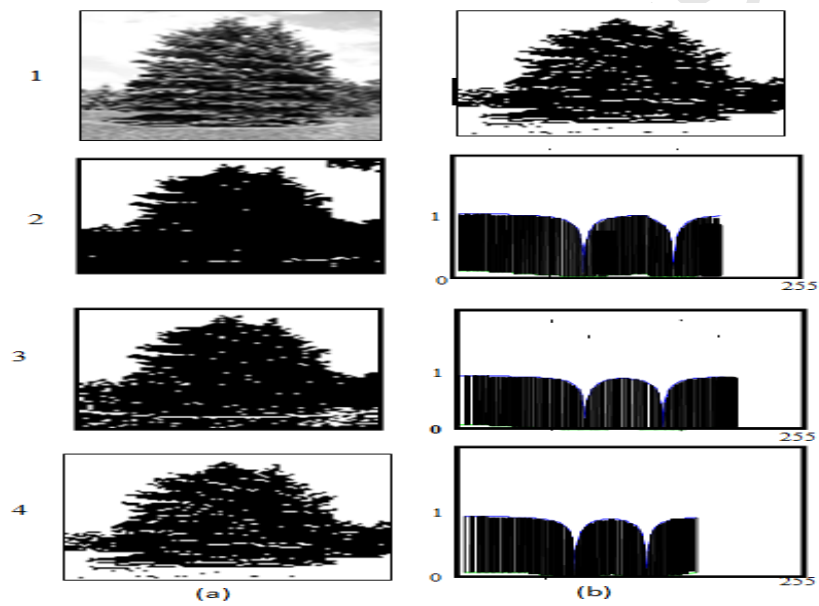


Figure 5: Row wise (1) Original test image(first column) from [46] and the corresponding ground truth (second column), (2),(3) and (4) are the segmentation results(first column) after 10, 15 and 20 generations and the corresponding IT2FMF (second column).

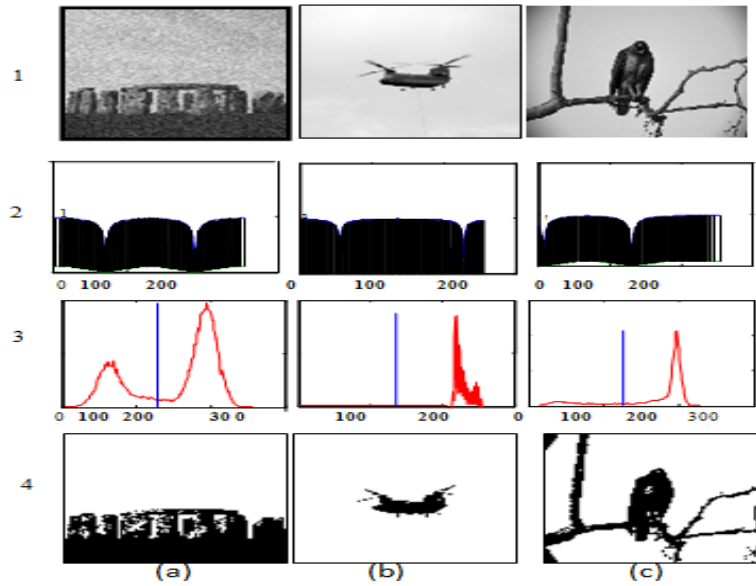


Figure 6: Row wise (1) Original test image (2) Exact IT2FMF of the segmented image (3) Histogram of the image with the position of threshold value. (4) Result using proposed method.



Figure 7: Some additional results by the proposed method. Row wise (1) Original test images (2) segmentation results by the proposed method

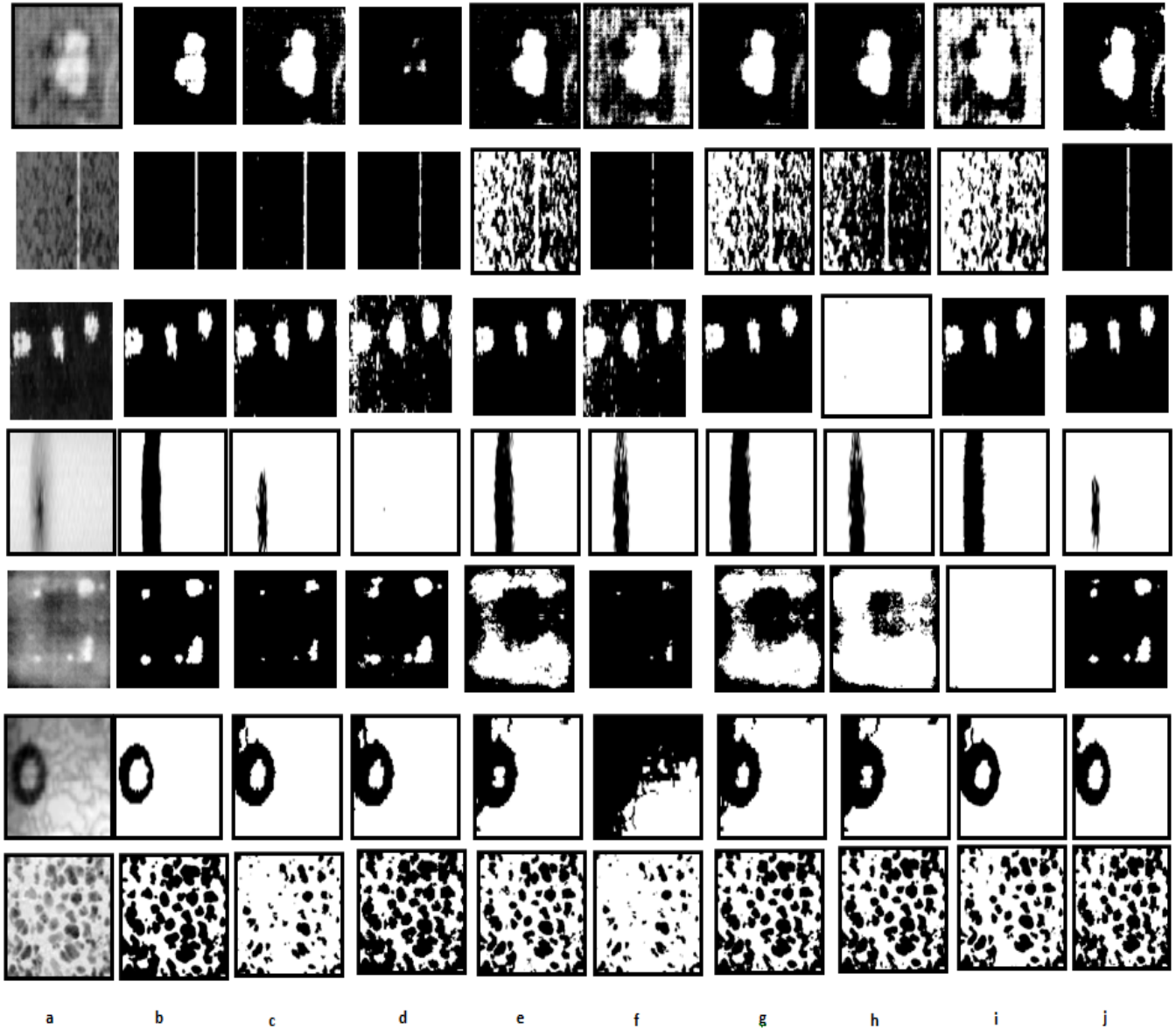


Figure 8: Column wise (a) Original NDT test image from [48] (b)Ground truth for segmentation result (c)Result using Kapur [7] (d) Result using Tizhoosh [24] (e) Results using Otsu [4] (f)Results using Huang [17] (g)Results using Ye [16] (h)Results using Pagola [25] (i)Results using Cai [5] (j)Results using proposed method

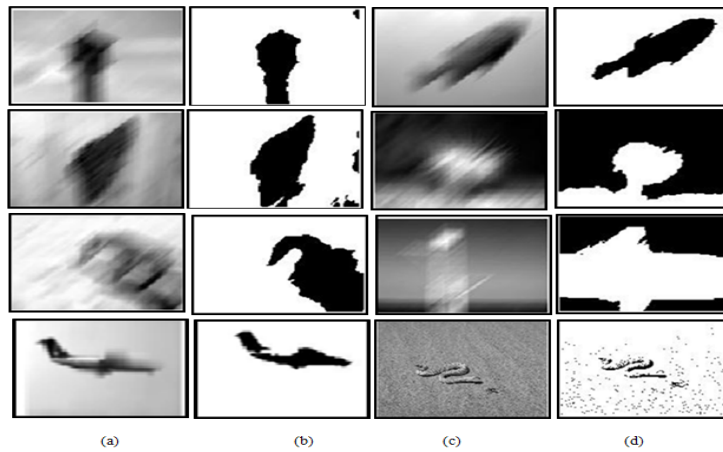


Figure 9: Segmentation results by the proposed method on the blurred images by Gaussian filter($\sigma = 4$). Column wise (a) Blurred test images (b) Segmentation by the proposed method. (c) Another set of blurred images (d) Segmentation by the proposed method

539 publicly available web sites were blurred using a Gaussian filter. The reason is that in
 540 a blurred image, the uncertainties increased. So, locating the segmentation boundary
 541 accurately became a difficult task. In Figure 9 some segmentation results on the blurred
 542 images are shown. The visual inspection shows that in almost all the blurred images,
 543 the segmentation boundary became exact. The reason is that, though uncertainties
 544 were increased in a blurred image, the adaptive uncertainty reduction with the changed
 545 statistics of the image helped to detect the boundaries properly.

546 9.5. Comparison of BA with Genetic algorithm and Particle Swam Optimization(PSO)

547 In this subsection we compared the BA with genetic algorithm(elitist model) [30]
 548 and an updated version of standard PSO called the MeanPSO [34]. To compare with
 549 the algorithms, we applied them on the same bag of type-1 membership functions to
 550 generate the IT2FMF of same image and calculated the threshold value. For genetic
 551 algorithms, we used the the mutation probability $p_m = 0.05$ and crossover probability
 552 of $p_c = 0.95$. For MeanPSO, we used the acceleration coefficients $c_1 = c_2 = 2$ and the
 553 inertia function $I = 1$. The quantitative result of each method was measured by taking
 554 the average of 30 runs. The quantitative results are shown in Table 2. From the result it

Table 2: Comparison with GA and MeanPSO

<i>Methods</i>	<i>Dataset</i>	<i>M.E</i>
<i>GA(Elitistmodel)</i>	<i>NDTimages</i>	0.0611
<i>MeanPSO</i>		0.0561
<i>BA</i>		0.0480
<i>GA(Elitistmodel)</i>	<i>Weizmann</i>	0.0600
<i>MeanPSO</i>		0.0543
<i>BA</i>		0.0434

555 can be seen that for generating the IT2FMF for segmentation, the BA is more efficient
 556 than that of GA and MeanPSO. The BA is superior to GA due to the fact that the BA
 557 takes into account the advantages of PSO and simulated annealing. Moreover, PSO is
 558 a special case of BA under appropriate simplifications.

559 10. Conclusions

560 In this paper, we have proposed an image thresholding method based on IT2FMF.
 561 The method generates the IT2FMF using a bag of type-1 membership functions de-
 562 pending on the statistics of the image at hand. The evolutionary Bat algorithm is used
 563 to judiciously find the optimal set of the membership functions from the bag and com-
 564 bine the different parameters of them to speed up the process. The method does not
 565 need any prior knowledge about the image and it does not require any external expert
 566 to select the membership functions. The IT2FMF generated in this way to achieve the
 567 object background segmentation result with higher accuracy in comparison to many
 568 existing and state-of-the-art techniques reported in the literature. It is to be noted the
 569 proposed method performed equally well for different types of images taken from stan-
 570 dard datasets. The method also showed robustness under the moderate noise corrup-
 571 tions compared to other methods. It is verified by the modified Cramer-Rao bound for
 572 the MSE. Moreover, the method performed well on the blurred image with uncertain
 573 boundaries. With suitable modification in the current method, it can be extended for
 574 the multiclass problem, which is being currently investigated.

575 **References**

- 576 [1] M. Sezgin and B. Sankur. Survey over image thresholding techniques and quan-
577 titative performance evaluation. *Journal of Electronic Imaging*, 13(1):146–165,
578 2004.
- 579 [2] Y. Bazi, L. Bruzzone, and F. Melgani. Image thresholding based on the em algo-
580 rithm and the generalized gaussian distributio. *Pattern Recognition*, 40:619–634,
581 2007.
- 582 [3] W.H. Tsai. Momment preserving thresholding: a new approach. *Computer Vision,*
583 *Graph and Image Processing.*, 29:377–393, 1985.
- 584 [4] N. Otsu. A threshold selection method from gray level histograms. *IEEE trans-*
585 *actions on System Man and Cybernatics.*, 9:62–66, 1979.
- 586 [5] H. Cai, Z. Yang, X. Cao, W. Xia, and X. Xu. A new iterative triclass thresholding
587 technique in image segmentation. *IEEE Transactions on Image processing.*, 23
588 (3):1038–1046, 2014.
- 589 [6] Y.K. Lai and P.L. Rosin. Efficient circular thresholding. *IEEE Transactions on*
590 *Image processing*, 23(3):992–1001, 2014.
- 591 [7] J.N. Kapur, P.K. Sahoo, and A.K.C. Wang. A new method for gray-level picture
592 thresholding using the entropy of the histogram . *Computer Vision, Graphics and*
593 *image processing.*, 29:273–285, 1985.
- 594 [8] M. Beauchemin. Image thresholding based on semivariance. *Pattern Recognition*
595 *Letters*, 34:456–462, 2013.
- 596 [9] Z. Hou, Q. Hu, and W.L. Nowinski. On minimum variance thresholding. *Pattern*
597 *Recognition Letters*, 27:1732–1743, 2006.
- 598 [10] T. Pun. A new method for grey-level picture threshoding using entropy of a
599 histogram. *Pattern Recognition.*, 19:41–47, 1986.

- 600 [11] J. Kittler and J. Illingworth. Minimum error thresholding . *Signal Process.*, 2:
601 223–237, 1980.
- 602 [12] M.K. Kundu and S.K. Pal. Thresholding for edge detection using human psycho-
603 visual phenomena. *Pattern Recognition Letters.*, 4:433–441, 1986.
- 604 [13] L. A. Zadeh. Quantitative fuzzy semantics. *Information science.*, 13:159–176.,
605 1971.
- 606 [14] S. K. Pal, R. A. King, and A.A. Hashim. Automatic grey level thresholding
607 through index of fuzziness and entropy. *Pattern Recognition Letters*, 1:141–146,
608 1983.
- 609 [15] S. K. Pal, D. Bhandari, and M. K. Kundu. Genetic algorithms for optimal image
610 enhancement. *Pattern Recognition Letters.*, 15:261–271, 1994.
- 611 [16] Z.W. Ye, M.N. Wang, W. Liu, and SB. Chen. Fuzzy entropy based optimal thresh-
612 olding using bat algorithm . *Applied soft computing.*, 23(3):992–1001, 2015.
- 613 [17] L.K. Huang and M.J. Wang. Image thresholding by minimizing the measure of
614 fuzziness. *Pattern Recognition*, 28:57–62, 1995.
- 615 [18] T. Chaira and A.K. Ray. Segmentation using fuzzy divergence. *Pattern Recogni-
616 tion Letters.*, 24:1837–1844, 2003.
- 617 [19] O.J. Tobias and R. Sear. Image segmentation by histogram thresholding using
618 fuzzy sets. *IEEE Transactions on Image processing*, 11(12):1467–1465, 2002.
- 619 [20] N. N. Karnik and J. M. Mendel. Introduction to type-2 fuzzy logic systems. *Pro-
620 ceeding of International Conference on Fuzzy Systems.*, pages 915–920., 1989.
- 621 [21] J. M. Mendel and R. I. B. John. Type-2 sets made simple. *IEEE Transactions on
622 Fuzzy Systems.*, 10:117–127., 2002.
- 623 [22] R. Hosseini, S. L. Qanadli, S. Barman, M. Mazinani, T. Ellis, and J. Dehmeshki.
624 An automatic approach for learning and tuning gaussian interval type-2 fuzzy
625 membership functions applied to lung cad classification system. *IEEE Trans-
626 actions on Fuzzy Systems.*, 20(2):224–234., 2012.

- 627 [23] J. M. Mendel. *Uncertain Rule-Based Fuzzy Logic Systems. Introduction and New*
628 *Directions*. . Englewood Cliffs, NJ: Prentice-Hall., 2001.
- 629 [24] H. Tizhoosh. Image thresholding using type-2 fuzzy sets. *Pattern Recognition*,
630 38:2363–2372, 2005.
- 631 [25] M. Pagola, C.L. Molina, J. Fernandez, E. Barrenechea, and H. Bustince. Intreval
632 type-2 fuzzy sets constructed from membership functions: Application to the fuzzy
633 thresholding algorithm. *IEEE transactions on Fuzzy systems*, 21(2):230–244,
634 2013.
- 635 [26] J.M. Mendel, R.I. John, and F. Liu. Interval type-2 fuzzy logic system made
636 simple. *IEEE transactions on Fuzzy systems*, 14(6):808–821, 2006.
- 637 [27] H. Tahayoriv, L. Livi, A. Sadeghian, and A. Rizzi. Interval type-2 fuzzy set
638 reconstruction based on fuzzy information-theoretic kernels. *IEEE Transactions*
639 *on Fuzzy Systems*, 23(4):1014–1029, 2015.
- 640 [28] T. W. Liao. A procedure for the generation of interval type-2 membership func-
641 tions from data. *Applied Soft Computing*, 52:925–936, 2017.
- 642 [29] T. W. Liao, A. K. Celmins, and R. J. Hammell. A fuzzy c-means variant for the
643 generation of fuzzy term sets. *Fuzzy Sets and Systems*, 135(2):241–257, 2003.
- 644 [30] D. Bhandari, C. A. Murthy, and S. K. Pal. Genetic algorithm with elitist model
645 and its convergence. *International Journal of Pattern Recognition and Artificial*
646 *Intelligence*., 10(06):731–747, 1996.
- 647 [31] T. Kurban, P. Civicioglu, R. Kurban, and E. Besdok. Comparison of evolutionary
648 and swam based computational techniques for multilevel color image segmenta-
649 tion . *Applied soft Computing*., 23:128–143, 2014.
- 650 [32] R. E. Precup, R. C. David, E. M. Petriu, S. Preitl, and M. B. Radac. Fuzzy
651 logic-based adaptive gravitational search algorithm for optimal tuning of fuzzy
652 controlled servo systems. *IET Control Theory and Applications*., 7(1):99–107,
653 2013.

- 654 [33] D. Azar, K. Fayad, and C. Daoud. A combined ant colony optimization and
655 simulated annealing algorithm to assess stability and fault-proneness of classes
656 based on internal software quality attributes. *International Journal of Artificial*
657 *Intelligence.*, 14(2):137–156, 2016.
- 658 [34] K. Deep and J. C. Bansal. Mean particle swarm optimisation for function opti-
659 misation. *International Journal of Computational Intelligence Studies.*, 01(01):
660 72–92, 2009.
- 661 [35] X.S. Yang. A new metaheuristic bat-inspired algorithm. *International journal of*
662 *Bio-inspired Computation*, 3(5):267–274, 2011.
- 663 [36] A.H. Gandomi, X.S. Yang, A.H. Alavi, and S. Talatahari. Bat algorithm for con-
664 strained optimization tasks . *Neural Computing and applications.*, 22(6):1239–
665 1255, 2012.
- 666 [37] X.S. Yang. Bat algorithm: literature ,review and applications . *International*
667 *journal of Bio-inspired Computation*, 5(3):141–149, 2013.
- 668 [38] T. W. Liao. Two hybrid differential evolution algorithm for engineering design
669 optimization. *Applied soft computing.*, 10(4):1188–1199, 2010.
- 670 [39] H. Bustince, E. Barrenechea, and M. Pagola. Restricted equivalence functions.
671 *Fuzzy Sets and Systems*, 157:2333–2346, 2006.
- 672 [40] H. Bustince, E. Barrenechea, and M. Pagola. Image thresholding using restricted
673 equivalence function and minimizing the measures of similarity. *Fuzzy Sets and*
674 *Systems.*, 158:496–516, 2007.
- 675 [41] E. Szmidt and J. Kacprzyk. Entropy for intuitionistic fuzzy sets. *Fuzzy sets and*
676 *systems*, 118(3):467–477, 2001.
- 677 [42] H. Zhang, J.E. Fritts, and S.A. Goldman. Image segmentation evaluation: A
678 survey of unsupervised methods. *Computer Vision and Image understanding .*,
679 110:260–280, 2008.

- 680 [43] Y. Zhang. A survey on evaluation methods for image segmentation. image seg-
681 mentation evaluation: A survey of unsupervised methods. *Pattern Recognition.*,
682 29:1335–1346, 1996.
- 683 [44] R. Peng and P.K. Varshney. On performance limit of image segmentation algo-
684 rithms. *Computer Vision and Image understanding*, 132:24–38, 2015.
- 685 [45] A. Alihodzic and M. Tuba. Framework for bat algorithm optimization meta-
686 heuristic. *Recent Researches in Medicine, Biology and Bioscience.*, 2011. ISBN:
687 978-960-474-326-1.
- 688 [46] <http://www.wisdom.weizmann.ac.il>.
- 689 [47] <https://www.eecs.berkeley.edu/Research/Projects/CS/vision/bsds/>.
- 690 [48] <http://mehmetsezgin.net>.

Highlights

- The method segments an image into object and background using interval type-2 fuzzy set.
- The interval type-2 fuzzy membership function is adaptively generated from a bag of type-1 membership function depending on the image statistics.
- Evolutionary Bat algorithm is used to increase the computational efficiency of the method.

Accepted Manuscript

Graphical abstract